

Understanding Fractures and Pore Compressibility of Shales using NMR

M. Dick¹, D. Green¹, E.M. Braun², and D. Veselinovic¹

¹*Green Imaging Technologies, Fredericton, NB, Canada*

²*Consultant, Houston, TX, USA*

This paper was prepared for presentation at the International Symposium of the Society of Core Analysts held in Snowmass, Colorado, USA, 21-26 August 2016

Abstract

For the profitable development of shale reservoirs, it is critical to understand the natural fractures in the rock and how they may or may not interact with hydraulic fracturing. When performing core analysis, it is also important to assess whether the measured properties have been altered by fractures induced during coring. A key indication of the quantity of the fractures can be obtained by measuring the amount of porosity contained in the fracture network. Shale pores are typically very small and therefore have very short NMR T₂ relaxation times. The fractures are larger than the pores and therefore have longer T₂ relaxation times.

In this work, we describe and demonstrate techniques using NMR that can obtain not only the total porosity of shale samples but can also quantify the amount of porosity arising from the fractures. Simple NMR measurements of the T₂ relaxation time were performed at different confining pressures to quantify the porosity loss as confining stress increases.

In some cases, porosity loss occurred preferentially in large pores at low confining pressure, suggesting fracture closure. The micropores did not respond to confining pressure, indicating that they were not part of the mechanical fabric of the rock. In another example, the lowest-T₂ peak dominated the NMR signal, indicating negligible porosity in fractures or large pores.

Introduction

NMR is widely used in the oil and gas sector to investigate both the types of fluids present and the size of the pores the fluids occupy [1]. Ignoring diffusion, the relationship between the NMR property T₂ and the pore size is governed by the following equation.

$$\frac{1}{T_2} = \frac{1}{T_{2-Bulk}} + \rho \frac{S}{V} \quad (1)$$

Where S/V is the surface to volume ratio of the pore, ρ is the relaxivity parameter and T_{2-bulk} is the T₂ relaxation time of the fluid.

In shale formations there usually exists at least two distinct pore networks [2,3]. One associated with the intergranular pore network and one associated with the pores within the organic rich kerogen. The fracture network, either natural or induced, could be thought of as a third pore network which at ambient pressure would be the largest in size.

Experiment

The total porosity and T_2 distribution as a function of confining pressure of four shale core samples was investigated using NMR. All samples were from wells drilled into potentially hydrocarbon-bearing rock formations. Characteristic information on each shale sample can be found in Table 1. The table includes the He porosity measured for the shales tested. Typically, in shales the He porosity is lower than the NMR porosity. Figure 1 shows a contrast enhanced photo of each shale tested. The natural color of the shale samples was dark brown and much of the heterogeneity shown in the figures was not visible before the contrast enhancement. Each dry shale sample was first vacuum saturated with brine (2% KCl in water) for approximately an hour. Saturation of the tight shale pores was then achieved by applying 10000 PSI pressure with brine for approximately a week in a Phoenix Instruments pressure vessel. It is assumed that this saturation procedure fully saturates all the mineral lined pores. However, it is unlikely that the kerogen pores are fully saturated after this procedure. But, these pores are extremely small and will not make a significant contribution to the total porosity measured. Following this saturation procedure, each shale sample was confined hydrostatically by fluorinert in an Oxford Instruments P5 overburden NMR probe [4]. Once the confined sample in the probe was free of leaks, it was inserted into an Oxford Instruments GeoSpec 2-53 rock core analyzer [5]. The porosity of each shale core sample was then tested as a function of confining pressure at 0, 1000, 2000, 3000, 4000 and 5000 PSI. A T_2 NMR acquisition scan of each sample at each pressure was used to measure the T_2 pore distribution as a function of confining pressure. The T_2 relaxation time is proportional to pore size. Data acquisition and data analysis of the T_2 data was achieved via Green Imaging Technology software [6].

Results

The pore-size distribution for each shale core sample tested at 5000 PSI of confining pressure can be seen in Figure 2. The data shown has not been background corrected. The total porosity of each shale could be determined by summing the area under its incremental porosity vs. T_2 curve. Figure 3 shows the total porosity of each shale normalized to 0 PSI as a function of confining pressure. Each of these shales shows an approximate five percent compression of their total porosity as the confining pressure is increased from 0 to 5000 PSI.

What is not obvious from Figure 3 is that the total porosity in each of the shales occurs in different pore networks in each shale sample. Shales 1 and 3 have a single sized pore network while shales 2 and 4 have three pore networks of varying size. For shale samples 2 and 4, the cumulative porosity of each network was estimated by summing the incremental porosity in certain T_2 ranges corresponding to the pore networks. The T_2 ranges for each pore network were determined by finding the minimum or inflection points between adjacent T_2 peaks. For example, in shale 2 the three pore networks were micro ($T_2 < 1.7$ ms), meso ($T_2 1.7-55$ ms) and macro ($T_2 > 55$ ms).

The left panel of Figure 4 shows the porosity of each pore network of shale 2 plotted as a function of confining pressure. This plot shows that the micro pore network makes up

the majority of the total porosity of shale 2 (~3 p.u.) while the macro porosity (~0.5 p.u.) accounts for the least portion of the total porosity of shale 2. The shape of each data for each pore network also gives some indication that each of the pore networks is behaving differently as the pressure is increased. This difference in behavior is enhanced in the center panel of Figure 4 where the porosity has been normalized to 0 PSI and plotted as a function of pressure. From the plot it is now immediately obvious that each pore network behaves differently with confining pressure. The micro pore network (blue line) shows no compression with confining pressure. The meso pore network (green line) shows an approximately linear compression with confining pressure. The macro pore network shows a sharp decrease in porosity from 0 to 1000 PSI and then no further compression from 1000 to 5000 PSI. This is consistent with the observations of Chhatre et al. [7]. In their study, there was a significant decrease in permeability with increasing stress, suggesting that the largest pores compacted the most. Finally, the right panel of Figure 4 shows the cumulative porosity of shale 2 as a function of confining pressure. Again it is obvious that the micro pores contribute to the majority of the total porosity of shale 2 while the macro pores contribute the least. However, the pressure dependence of the cumulative porosity masks the unique behavior of the porosity of each pore network.

Figure 5 shows the porosity data for shale 4 analyzed in the same fashion as the data for shale 2. This plot shows that for shale 4, the meso pore network makes up the majority of the total porosity (~5 p.u.) while the macro porosity (~0.5 p.u.) accounts for the least portion of the total porosity. The center panel of Figure 5 shows the porosity normalized to 0 PSI and plotted as a function of pressure. This plot shows that there is consistency with shale 2 for the behavior of the micro, meso and macro pore networks as a function of pressure. Finally, the right panel of Figure 5 shows the cumulative porosity of shale 4 as a function of confining pressure. Again it is obvious that the meso pores contribute to the majority of the total porosity of shale 2 while the macro pores contribute the least. However, the pressure dependence of the cumulative porosity masks the unique behavior of the porosity of each pore network

Technique customization

The measurements reported here were intended as a feasibility study, and followed identical protocols for all samples. For application to specific field development studies, it is expected that experimental protocols could be customized. Some options include:

- Changing net confining stress by reducing pore pressure, to more closely duplicate conditions during field development.
- Monitoring T_2 relaxation times over time to study stress creep.
- Measuring permeability changes in conjunction with T_2 relaxation times.
- Correlating compressibility behavior with other rock properties such as mineralogy, geologic facies, kerogen content, etc.

Conclusion

A method has been presented for using NMR T_2 relaxation times to identify pore networks in shales and their dependence on stress. Four samples were tested, all taken

from wells in potential hydrocarbon-bearing formations. Two samples had a complex (trimodal) pore size distribution, and two contained only very small pores.

Where a complex distribution was present, the stress-dependence varied by pore size. The largest (macro) pores compressed significantly at relatively low stress (1000 psi), and very little thereafter. We interpret this to indicate the closure of natural or induced fractures. The smallest (micro) pores show no significant change with stress. We interpret this to indicate that these pores are not part of the mechanical fabric of the rock. The intermediate size (meso) pores show a continuing compression across the range of stresses.

References:

1. Coates, G.R., Xiao, L., and Prammer, M.G., *NMR Logging. Principles & Applications*, Halliburton Energy Services, Houston, 1999.
2. Kausik, R., Fellah, K., Rylander, E., Singer, P., Lewis, R., and Sinclair, S., NMR Relaxometry in Shale and Implications for Logging, SPWLA 56th Annual Logging Symposium, July 18-22, 2015.
3. Suarez-Rivera, R., Chertov, M., Willberg, D. M., Green, S. J., & Keller, J. (2012, January 1). Understanding Permeability Measurements in Tight Shales Promotes Enhanced Determination of Reservoir Quality. Society of Petroleum Engineers. doi:10.2118/162816-MS.
4. P5 Overburden Probe User Manual, Version 1, Oxford Instruments, Green Imaging Technologies.
5. Geo-Spec 2-53 User Manual, Version 1.8, Oxford Instruments.
6. GIT Systems and LithoMetrix User Manual, Revision 1.9, Green Imaging Technologies.
7. Chhatre, S.S., Braun, E.M., Sinha, S., Determan, M.D., Passey, M.D., Zirkle, T.E., Wood, A.C., Boros, J.A., Berry, D.W., Leonardi, S.A. and Kudva, R.A., Steady State Stress Dependent Permeability Measurements Of Tight Oil Bearing Rocks, 2014 Annual Symposium Of The Society Of Core Analysts (SCA2014- 012).

Tables and Figures:

Table 1: Characteristic Information On Shale Samples Tested

Shale	1	2	3	4
Formation	Gates	Doig	Muskwa	Montney
Sample Depth (ft)	1392	5256	5422	6538
Core Diameter (cm)	2.5	2.5	2.5	2.5
Core Length (cm)	3.8	3.9	4.4	4.3
Bulk Volume (cm ³)	18.7	19.1	21.6	21.1
Dry Core Mass (g)	51.68	51.2	55.0	54.8
Grain Density (g/cc)	2.74	2.68	2.61	2.72
Gas Permeability (mD)	4.28	1.3	0.301	5.18
He Porosity (p.u.)	5.9	5	7.4	8.9
Well Location	British Columbia	British Columbia	British Columbia	British Columbia

Figure 1: Contrast-enhanced photographs of the shale samples tested

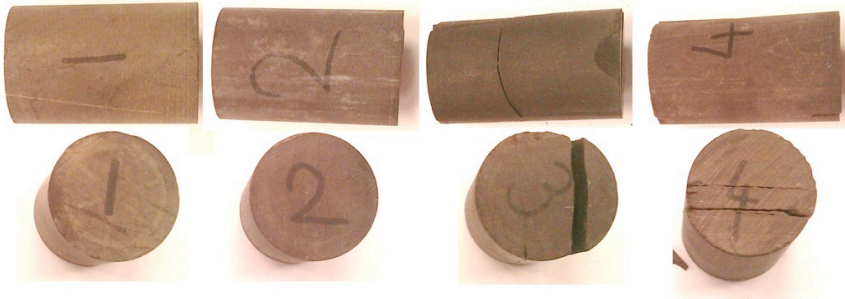


Figure 2: Pore Distribution For Shale Samples Tested At 5000 PSI Confining Pressure.

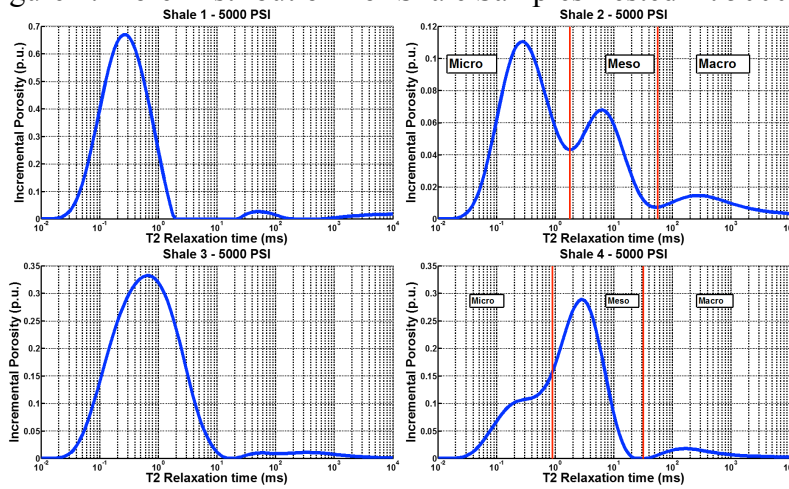


Figure 3: The Porosity (Normalized to 0 PSI) Of Shales 1-4 As A Function Of Confining Pressure

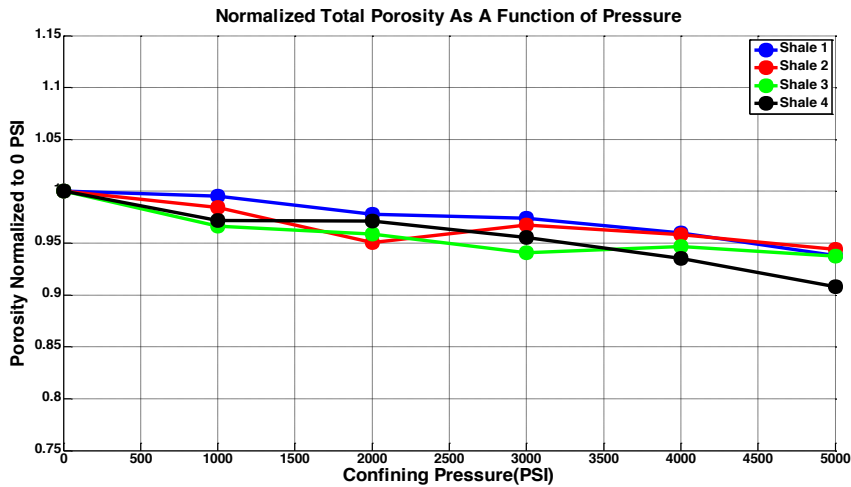


Figure 4: The Porosity Of The Pore Networks Of Shale 2 As A Function Of Pressure

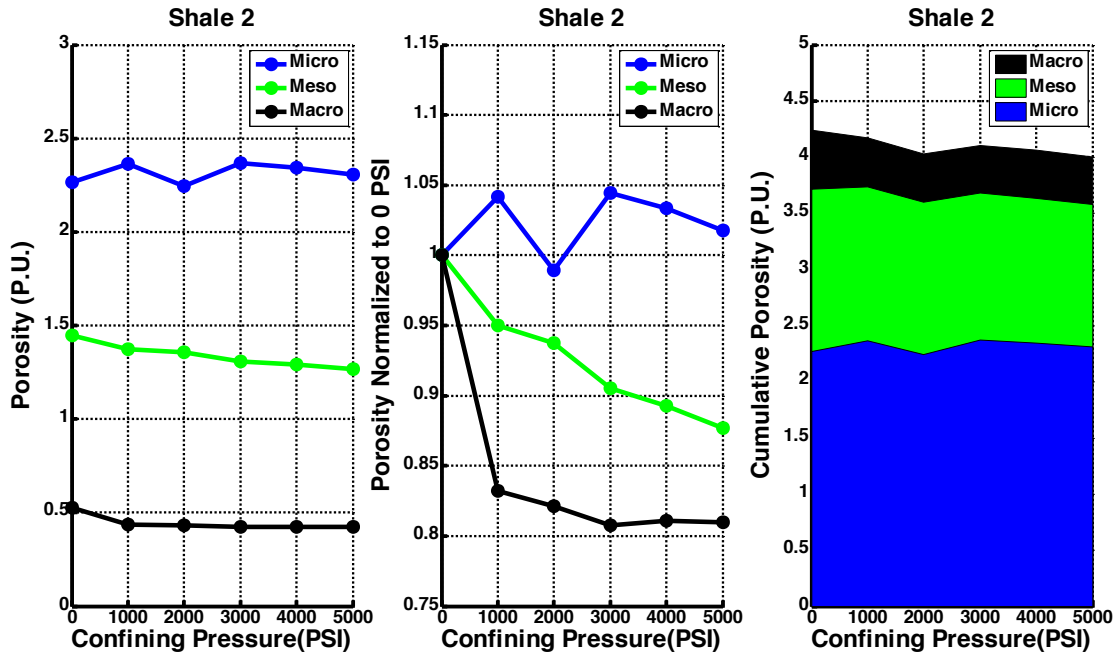


Figure 5: The Porosity Of The Pore Networks Of Shale 4 As A Function Of Pressure

